The Abdus Salam
International Centre for Theoretical Physics

United Nations
Educational, Scientific and
Cultural Organization

IAEA
International Atomic Energy Agency

2036-3

International Workshop: Quantum Chromodynamics from Colliders to Super-High Energy Cosmic Rays

25 - 29 May 2009

Implications of Pomeron Enhancement at Extremely High Energies

Uri Maor

Telaviv University
Telaviv
Israel

Strada Costiera 11, 34014 Trieste, Italy - Tel. +39 040 2240 111; Fax +39 040 224 163 - sci_info@ictp.it, www.ictp.it

Implications of Pomeron Enhancement at Extremely High Energies

Uri MAOR
Tel-Aviv University

Multi Pomeron interactions have a profound implications on soft scattering cross sections and survival probabilies of LRG at extremely high energies. I shall discuss this phenomenon checking the dependence of its predictions on the input modeling and parameters. I shall concentrate on recent Multi channel models: Gotsman, Levin, Maor, Miller - GLM(07), GLM(08), GLMM(09).
Khoze, Martin, Ryskin, Luna - KMR(07), LKMR(08) KMR(08), KMR(09). I shall refer also to Frankfurt, Hyde, Strikman, Weiss - FHSW(07,08,09).

1. Introduction

The renewed interest in soft scattering and Pomeron physics is correlated to the market demands for reliable estimates of hard diffraction gap survival probabilities, notably Higgs production at the LHC.

Low mass Higgs production in exclusive central diffraction, preferably coupled to forward tagging of the outgoing protons, has a very good discovery potential provided S_H^2, its gap survival probability, is not too small.

This is the background of the disagreement between Tel Aviv and Durham. Even though the GLMM and KMR models are conceptually similar, their final predictions are very different

$$\frac{S_H^2(KMR)}{S_H^2(GLMM)} = \frac{0.015}{0.0025} = 6.$$

The output of FHSW is compatible with GLMM.

As we shall see the significant differences between GLMM and KMR are traced to distinctly different modellings and data analysis.

The seemingly confined S^2_H calculation touches on a few fundamental issues:

- The role of s and t channel unitarity and the consequent quest for experimental signatures implied by the above.
- The nature of the Pomeron and its QCD formalism. What is the relation between soft and hard Pomerons?
- Is the triple Pomeron coupling a fundamental entity without which we can not understand the high energy regeme of strong interactions? What is the roll of multi Pomeron interactions?
- Implementing unitarity is not a unique procedure, and is, thus, model dependent. Hence, constructing a unitarity compatible model intimately depends on an interplay between theory, modelling and data.
- What can we learn from the approach of the elastic amplitude to the black disc bound at small impact parameter b?
- How much diffraction do we expect at exceedingly high energies? What are the consequences for σ_{tot}, σ_{el} and S^2_{diff}?

1.3

	Tevatron			LHC			W=10^5 GeV		
	GLMM	KMR(07)	KMR(08)	GLMM	KMR(07)	KMR(08)	GLMM	KMR(07)	KMR(08)
σ_{tot}(mb)	73.3	74.0	73.7	92.1	88.0	91.7	108.0	98.0	108.0
σ_{el}(mb)	16.3	16.3	16.4	20.9	20.1	21.5	24.0	22.9	26.2
σ_{sd}(mb)	9.8	10.9	13.8	11.8	13.3	19.0	14.4	15.7	24.2
$\sigma_{sd}^{\text{low M}}$	8.6	4.4	4.1	10.5	5.1	4.9	12.2	5.7	5.6
$\sigma_{sd}^{\text{high M}}$	1.2	6.5	9.7	1.3	8.2	14.1	2.2	10.0	18.6
σ_{dd}(mb)	5.4	7.2		6.1	13.4	?	6.3	17.3	
$\frac{\sigma_{el}+\sigma_{diff}}{\sigma_{tot}}$	0.43	0.46		0.42	0.53	?	0.41	0.57	
S^2_{2ch}(%)	5.3	1.8-4.8		4.0	1.2-3.2	4.5	3.45	0.9-2.5	
S^2_{enh}(%)	28.5	100		6.3	100	33.3	3.3	100	
S^2(%)	1.5	2.7-4.8		0.25	1.2-3.2	1.5	1.15	0.9-2.5	

TABLE III: Comparison of GLMM, KMR(07) and KMR(08) outputs.

2. The Good-Walker Eikonal Models

Updated eikonal models are multichannel, taking into account both elastic and diffractive re-scatterings. This is a consequence of the Good Walker mechanism.

Consider a system with 2 states: a hadron $|h\rangle$ and a diffractive system $|D\rangle$. The GW mechanism stems from the observation that these states do not diagonalize the 2x2 scattering matrix T. Define the eigen states of T by $|\psi_1\rangle$ and $|\psi_2\rangle$. We obtain

$$\psi_h = \alpha\psi_1 + \beta\psi_2 \qquad \alpha^2+\beta^2=1$$
$$\psi_D = -\beta\psi_1 + \alpha\psi_2$$

In this representation we consider 4 elastic scatterings of ψ_i and ψ_k $(i,k=1,2)$: $A_{i,k} = \langle\psi_i\psi_k|T|\psi_i\psi_k\rangle$.

In pp and $\bar{p}p$ scattering $A_{1,2}=A_{2,1}$ and we have 3 independent amplitudes which are the building blocks of:

$$A_{i,k} = A_{i,k}(s,b) \left\{ \begin{aligned} a_{el}(s,b) &= i\,\{\alpha^4 A_{1,1} + 2\alpha^2\beta^2 A_{1,2} + \beta^4 A_{2,2}\} \\ a_{sd}(s,b) &= i\alpha\beta\,\{-\alpha^2 A_{1,1} + (\alpha^2-\beta^2)A_{1,2} + \beta^2 A_{2,2}\} \\ a_{dd}(s,b) &= i\alpha^2\beta^2\,\{A_{1,1} - 2A_{1,2} + A_{2,2}\} \end{aligned} \right.$$

Specification of a_{el}, a_{sd} and a_{dd} enables us to calculate through a b integration the total cross section and the differential and integrated elastic, SD and DD cross sections.

For each of the $A_{i,k}$ amplitudes we write its unitarity equation $\mathrm{Im}\, A_{i,k}(s,b) = |A_{i,k}(s,b)|^2 + G^{in}_{i,k}(s,b)$. i.e. for each i,k

$$\sigma^{i,k}_{tot}(s,b) = \sigma^{i,k}_{el}(s,b) + \sigma^{i,k}_{in}(s,b)$$

A general solution can be written as $A_{i,k} = i\left(1 - e^{-\frac{1}{2}\Omega_{i,k}}\right)$
$G^{in}_{i,k} = 1 - e^{-\frac{1}{2}\Omega_{i,k}}$. In the eikonal approximation we assume that $A_{i,k}(s,b)$ is imaginary (i.e. $\Omega_{i,k}$ is real). $\Omega_{i,k}(s,b)$ is determined by the input model.

$\Rightarrow$ $P_{i,k}(s,b) = e^{-\Omega(s,b)}$ is the probability that the GW (i,k) projectiles will reach the final non GW interaction in their initial state, regardless of their prior re-scattering.

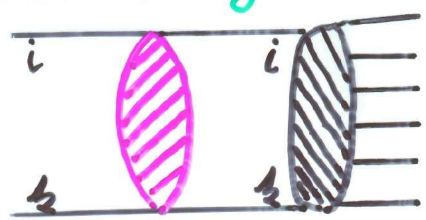

Eikonal models based on the GW mechanism use a Regge like formalism in which the soft Pomeron trajectory is $\alpha_{I\!P}(t) = 1 + \Delta_{I\!P} + \alpha'_{I\!P}\, t$. The corresponding opacity is $\Omega_{i,k}(s,b) = \nu_{i,k}(s)\, \Gamma_{i,k}(s,b;\alpha'_{I\!P})$ where $\nu_{i,k} = g_i\, g_k \left(\frac{s}{s_0}\right)^{\Delta_{I\!P}}$.

$\Gamma_{i,k}$ are the b-profiles of the (i,k) elastic scatterings.

Recall that $e^{-x} = x - \frac{x^2}{2!} + \frac{x^3}{3!} - \dots$ $(i,k = 1,2)$. Consequently

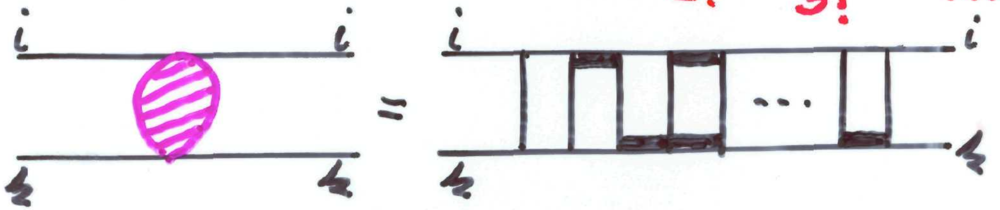

. $\Gamma_{i,k}(s,b)$ is external information derived from a fit to the soft scattering data, essentially the differential cross sections.

In GLMM(08) the b-profiles are given by a 2-pole in t-space

$$\Gamma_{i,k}(t;m_i,m_k) = \frac{1}{(1-t/m_i^2)} \times \frac{1}{(1-t/m_k^2)} \Longrightarrow \Gamma_{i,k}(b;m_i,m_k)$$

to which we introduce a mild energy dependence

$$m^2 \Longrightarrow m^2(s) = \frac{m^2}{1 + \frac{m^2}{4}\alpha'_{I\!P} \ln\frac{s}{s_0}}.$$

This parametrization is compatible with the requirements of analiticity/crossing at large b, pQCD at large t, Regge at small t.

KMR b-profiles are formulated some what differently than ours, but numerically they are similar.

Consider a model in which diffraction is exclusively GW. This was recently considered by GLM(08), GLMM (09) and LKMR (08). All these GW models fit their (different!) elastic sectors of their data bases with $\frac{\chi^2}{d.o.f} < 1.0$ with fitted $\Delta_{I\!P} = 0.10 - 0.12$ and $\alpha'_{I\!P} = 0.012 - 0.066$.

The above GW models fail to reproduce the diffractive sectors of their data base. This deficiency is traced to high mass diffraction which is mostly non GW.

3. Multi Pomeron Interactions

- Mueller (1969) triple Pomeron diagram (derived from 3 body unitarity)

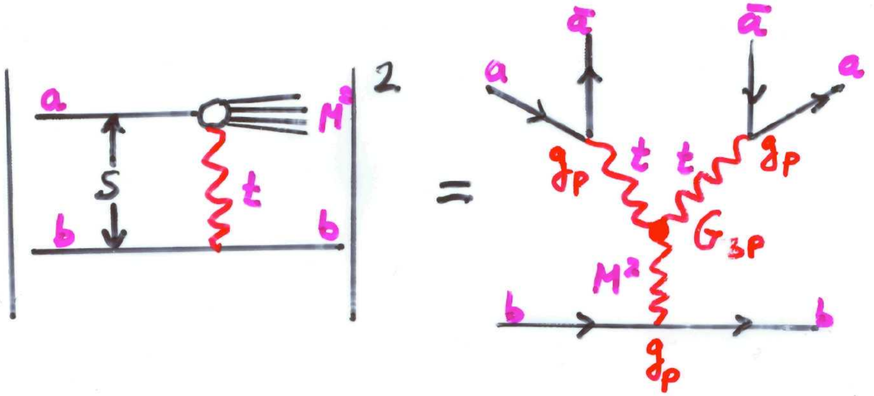

leads to high mass diffraction which is non GW. Recall that

$\frac{M^2}{s} \leq 0.05$ (commonly used but arbitrary)

The approximation requires that $M^2 \gg m_p$.

$$M^2 \frac{d\sigma^{3P}}{dt\, dM^2} = \frac{1}{16\pi^2} g_P^2(t)\, g_P(0)\, G_{3P}(t) \left(\frac{s}{M^2}\right)^{2\Delta_P + 2\alpha_P' t} \left(\frac{M^2}{s_0}\right)^{\Delta_P} + \text{secondary terms}$$

- CDF analysis suggests a relatively high value of G_{3P}.
- Assume G_{3P} is not too small $\Rightarrow$ we need to consider a very large family of multi Pomeron interactions ($\mathbb{P}$ enhancement) which are not included in the GW mechanism.
- As we shall see, this "new" dynamical mechanism initiates profound differences in the calculated values of soft diffractive cross sections and survival probabilities of non GW diffractive channels (soft and hard). These differences are significant at high energies above the Teratron !!!

	$\Delta_{I\!P}$	β	$\alpha'_{I\!P}$	g_1	g_2	m_1	m_2	$\chi^2/d.o.f.$
GW	0.120	0.46	0.012 GeV^{-2}	1.27 GeV^{-1}	3.33 GeV^{-1}	0.913 GeV	0.98 GeV	0.87
GW+$I\!P$-enhanced	0.335	0.34	0.010 GeV^{-2}	5.82 GeV^{-1}	239.6 GeV^{-1}	1.54 GeV	3.06 GeV	1.00

TABLE I: Fitted parameters for GLMM(08) GW and GW+$I\!P$-enhanced models.

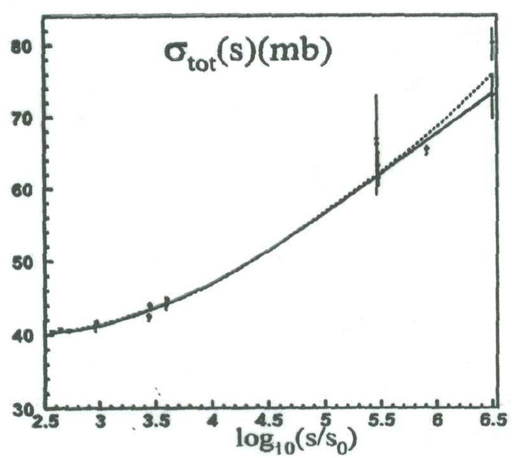

Figure 1: Energy dependence of σ_{tot}. The solid line shows the fit with taking into account all Pomeron interactions while the dashed line corresponds to two channel (eikonal) model.

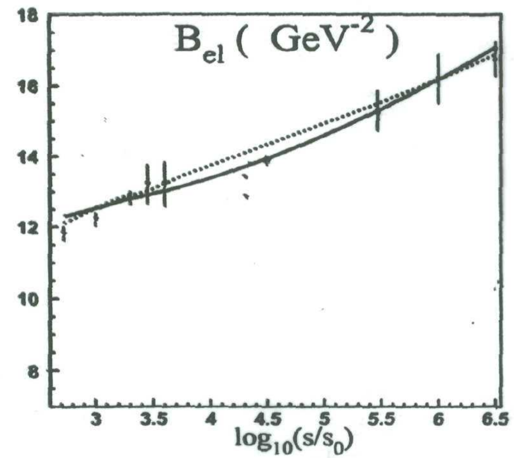

Figure 2: Energy dependence of the slope for the differential elastic cross section. All notation are the same as in Fig. 1

As noted, the Tel-Aviv and Durham models are conceptually similar. Both utilize multi channel eikonal models so as to be compatible with s-channel unitarity and multi Pomeron interactions so as to be compatible with t-channel unitarity. Their output, though, is significantly different reflecting both different modellings and data analysis.

4. Same Concept - Different Models

GLMM(08) and KMR(07) treatment of multi-Pomeron interactions (Pomeron enhanced) stems from a few clasical papers on this subject notably Kaidalov, Ponomarev, Ter-Martirosyan (1986). At the core of these papers is Gribov's Reggeon Calculus and its partonic interpretation. Recall that in our context the soft Pomeron is a simple pole in the J-plane, while the hard (BFKL) Pomeron is a branch cut.

KMR (07) derives directly from these foundations. At the foundation of the KMR(07) model are 2 ad hoc assumptions.

1) The coupling of a multi Pomeron point vertex $n\mathbb{P} \to m\mathbb{P}$ $(n+m \geq 3)$ is $g^n_m = \frac{1}{2} g_N \, nm \, \lambda^{n+m-2}$ $(n+m \geq 3)$. In this notation $G_{3P} = \lambda g_N$.

This assumption is not supported by either decisive data or a theoretical proof and it is justified by claiming it is "reasonable". Note that in Kaidalov et.al. $g^n_m = \frac{1}{2} g_N \lambda^{n+m-2}$, i,e. it is considerably smaller. High order g^n_m couplings are needed to avoid pathalogical reduction of Δ_P below 1. I shall discuss it in conjunction to the GLMM model.

2) Most of LHC non GW diffractive reaction of interest are hard. Given a triple $I\!P$ bare coupling  we recall that $G_{3I\!P}$ was originally defined for 3 soft $I\!P$. KMR assume that G_{3P} does not change by the interchange of soft → hard. This is not self evident.

The key observation of GLMM(08) is that the exceedingly small fitted $\alpha'_{I\!P} = 0.01\ GeV^{-2}$ implies that the "soft Pomeron" is hard enough to be treated perturbatively. Following Gribov we identify a correlation between $\alpha'_{I\!P}$ and $<P_t>$, the mean transverse momentum of the partons (actually colour dipoles) associated with the $I\!P$. Recall that the smallness of $\alpha'_{I\!P}$ is a general feature of GLMM and KMR models.

	GLMM(07)	KMR(07)	KMR(08)
$\Delta_{I\!P}$	0.335	0.55	0.30
$\alpha'_{I\!P}$	0.010	0	0.05

GLMM(08) : $<P_t> = 1/\sqrt{\alpha'_{I\!P}} \simeq 10\ GeV$

$\Rightarrow$ QCD running coupling constant is small enough to enable a pQCD calculation. $\alpha_s \propto \ln\left(<P_t^2>/\Lambda^2_{QCD}\right) \ll 1$.

Technically, we have adopted the pQCD MPSI procedure. In this summation g_m^n is reduced to a sequence of triple $I\!P$ vertexes (Fan diagrams). For this calculation we need to calculate the probabilities for $I\!P \to 2I\!P$ (pair production) and $2I\!P \to I\!P$ (annihilation).

Given the input $\alpha_{I\!P}(t) = 1 + \Delta_{I\!P} + \alpha'_{I\!P} t$ it is evident that s-channel unitarity corrections are needed. The question is at what energies these corrections become significant.

Recall that with no unitarity screening corrections

$$\sigma_{tot} \propto s^{\Delta_{I\!P}} \quad \text{and} \quad B_{el} = B_0 + 2\pi\alpha'_{I\!P} \ln\frac{s}{s_0}$$

In this simple picture $\Delta_{I\!P}$ controls the energy dependence of σ_{tot} and $\alpha'_{I\!P}$ the shrinkage of the forward elastic peak.

It is well known that in the ISR – Tevatron range, the DL simple parametrization provides an excellent reproduction of σ_{tot}, σ_{el}, B_{el} with $\Delta_{I\!P} = 0.08$ and $\alpha'_{I\!P} = 0.25\ GeV^{-2}$.

s-channel unitarity screening is required even at this energy range so as to explain the very mild energy dependence of SD and DD cross sections. Note that simple eikonal models with $0.12 \leq \Delta_{I\!P} \leq 0.18$ reproduce the ISR – Tevatron total and elastic data with $\Delta_{I\!P}^{eff} \simeq 0.08$.

More over, in these models $\sigma_{tot} \propto \ln^2\frac{s}{s_0}$ asymptotically.

However, the approach to the logarithmic behaviour is very very slow!!!

In general, the output dependences of σ_{tot}, σ_{el}, B_{el} on energy are obtained in eikonal models through a balanced act between Δ_{P} and $\alpha'_{I\!P}$ inputs. The smaller $\alpha'_{I\!P}$ gets a larger $\Delta_{I\!P}$ is needed and vice versa.

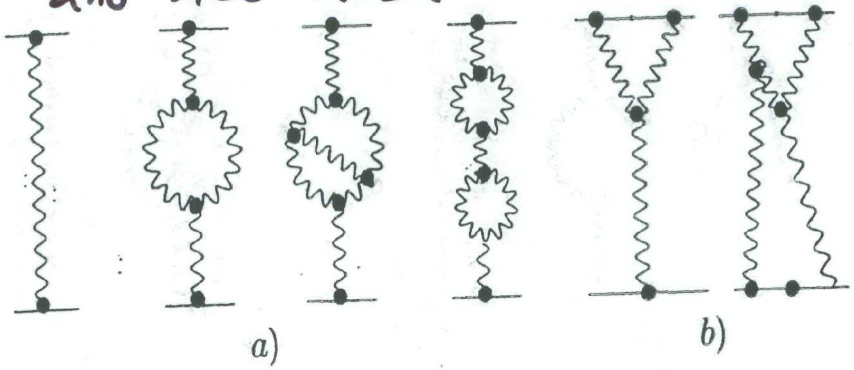

FIG. 1: Typical low order terms of the Pomeron Green's function. Enhanced Pomeron diagrams are shown in Fig. 1a, whereas Fig. 1b shows semi-enhanced diagrams which are not included in our calculations as yet.

Multi Pomeron interactions initiated by t-channel unitarity are essential so as to reproduce large mass diffraction in SD and DD. However, part of the multi Pomeron deal is a re-normalization of the $I\!P$ propagator through Pomeron loops.

The net result is a reduction of the output values of $\Delta_{I\!P}^{eff}$. This is general property observed in all the eikonal models I have considered.

	$\Delta_{I\!P}$ input	$\Delta_{I\!P}^{eff}$ 1.8–14	$\Delta_{I\!P}^{eff}$ 14–100	σ_{tot} LHC	σ_{el} LHC
GLM(07)	0.15	0.085	0.079	110.5	25.3
GLMM(08)	0.335	0.056	0.041	92.1	20.9
KMR(07)	0.55	0.042	0.027	88.0	20.1
KMR(08)	0.30	0.053	0.042	91.7	20.9
LKMR(09)	0.121	0.064		95.0	

Alan Martin has been very critical of the GLMM model presenting his opinion in several meetings over the last 2 years. According to him the lack of explicit b-dependence in MPSI approximation and the lack of direct point like multi Pomeron couplings in which $n+m>3$, contradict the asymptotic dependence of σ_{tot} in the $s\to\infty$ limit obtained from general principles. Specifically, $\Delta_{\mathbb{P}}^{eff}$ becomes negative at high enough energies. Regardless of the technical details, Alan's claim is conseptually non relevant! We have no tools to predict the functional transition from pre asymptotic to asymptotic energies. Both the GLMM and KMR have a bound of validity at $W=100$ TeV. This bound is a consequence of both groups executing their calculations with $\alpha'_{\mathbb{P}}=0$ (which is a more severe crime than what we are accused of). As it stands

$\Delta_{\mathbb{P}}^{eff}(GLMM(08)) > \Delta_{\mathbb{P}}^{eff}(KMR(07))$ and $\Delta_{\mathbb{P}}^{eff}(GLMM(08)) \gtrsim \Delta_{\mathbb{P}}^{eff}(KMR(08))$.

The above holds up to $W=100$ TeV.

5. The Interplay Between Theory and Data Analysis

There is a significant difference between GLMM and KMR data analysis. This reflects on both the construction of the two data base sets and the coupled free parameters adjustment.

The starting point of both investigations is the realization that a GW model reproduces the elastic data well, but the reproduction of the diffractive data is poor. Both groups claim to achieve a much improved reproduction of their respective data bases once $\mathbb{P}$-enhanced diagrams were added.

The meager data in the $Sp\bar{p}S$ – Tevatron range is not sufficient to constrain the $\mathbb{P}$ parameters. GLMM(08) and LKMR(09) chose, therefore, to extand their data base down to ISR ($W > 20$ GeV). This requires a $\mathbb{P}+\mathbb{R}$ fit from which one isolates the relevant $\mathbb{P}$ parameters. KMR (07,08) chose to tune rather than fit $\Delta_{\mathbb{P}}$ and $\alpha'_{\mathbb{P}}$ in a $\mathbb{P}$ only model.

GLMM data base has 55 points of σ_{tot}, σ_{el}, σ_{sd}, σ_{dd} and B_{el} in the ISR – Tevatron range. We add a consistency check of B_{sd} and $\frac{d\sigma_{el}}{dt}$ ($t \le 5$ GeV^2), $\frac{d\sigma_{sd}}{dt\, d\frac{M^2}{s}}$ at $t = 0.05$ GeV^2 (CDF). The reason: we did not wish to bias the fit by too many differential cross sections points.

As stated, the GLMM fit was done twice, once for GW and

	$\Delta_{I\!P}$	β	$\alpha'_{I\!P}$	g_1	g_2	m_1	m_2	$\chi^2/d.o.f.$
GW	0.120	0.46	0.012 GeV^{-2}	1.27 GeV^{-1}	3.33 GeV^{-1}	0.913 GeV	0.98 GeV	0.87
GW+$I\!P$-enhanced	0.335	0.34	0.010 GeV^{-2}	5.82 GeV^{-1}	239.6 GeV^{-1}	1.54 GeV	3.06 GeV	1.00

TABLE I: Fitted parameters for GLMM(08) GW and GW+$I\!P$-enhanced models.

again for GW+ P-enh. As seen $\alpha'_{I\!P}$ is very stable. The other free parameters change significantly. Noteably, $\Delta_{I\!P}$ is much higher. This is a consequence of the additional constraints implied by the diffractive data which is more screened than the elastic sector. Another significant change is $g_2(GW+P\text{-enh.}) \simeq 40\, g_2(GW)$.

The conceptual approach of KMR is completely different. Their data base contains just:

$\frac{d\sigma_{el}}{dt}$ ($t \leq 0.5\ GeV^2$) in the 60-1800 GeV range.

The corresponding σ_{tot}.

CDF $\frac{d\sigma_{sd}}{dt\, d\frac{M^2}{s}}$ at $t = 0.05\ GeV^2$.

In the KMR procedure the first stage is to fit/tune $\frac{d\sigma_{el}}{dt}$ including the consequent σ_{tot} so as to determine the b-profiles and the GW amplitudes. These are frozen and utilized in the second stage in which $\Delta_{I\!P}$, $\alpha'_{I\!P}$ are determined.

One of the consequences of the KMR procedure is that g_1 and g_2 are of the same order (compatible with GLMM first phase fit). As we shall see this output is critical in the study of the approach of $a_{el}(s,b)$ to the black disc bound.

Some, but not all, of the deficiencies of the KMR data analysis are amended in LKMR(09) in which both $\mathbb{P}+\mathbb{R}$ exchanges are included enabling a larger data base containing the ISR – Tevatron data. Recall, though, that LKMR have adopted the KMR approach and their data base contain only $\frac{d\sigma_{el}}{dt}$, σ_{tot} and $\frac{d\sigma_{sd}}{dt\,d\frac{M^2}{s}}$.

In my oppinion fitting $\frac{d\sigma_{el}}{dt}$ on its own is no more than a consistency check. KMR and LKMR data analysis has no resolution to determine the $\mathbb{P}$ parameters and the GW scattering amplitudes.

KMR(00) GW

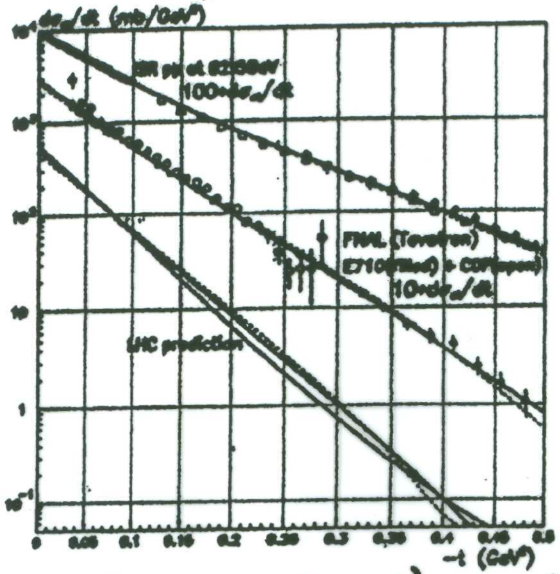

$\Delta_{I\!P} = 0.102 \quad \alpha'_{P} = 0.066$

RMK(07)

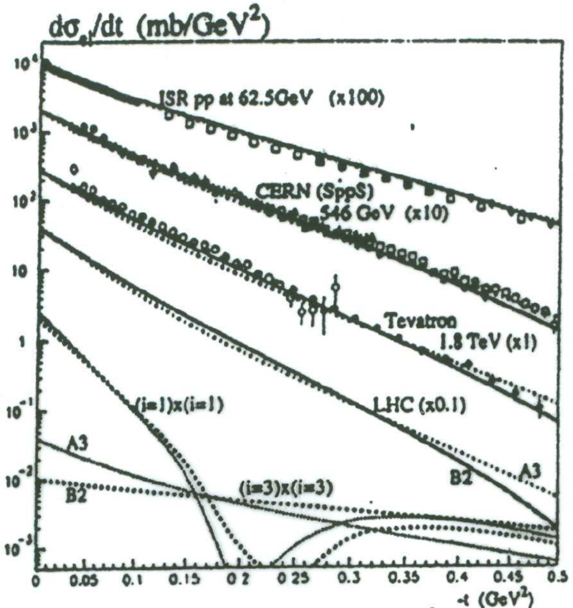

$\Delta_{I\!P} = 0.55 \quad \alpha'_{I\!P} \equiv 0$

RMK(08)

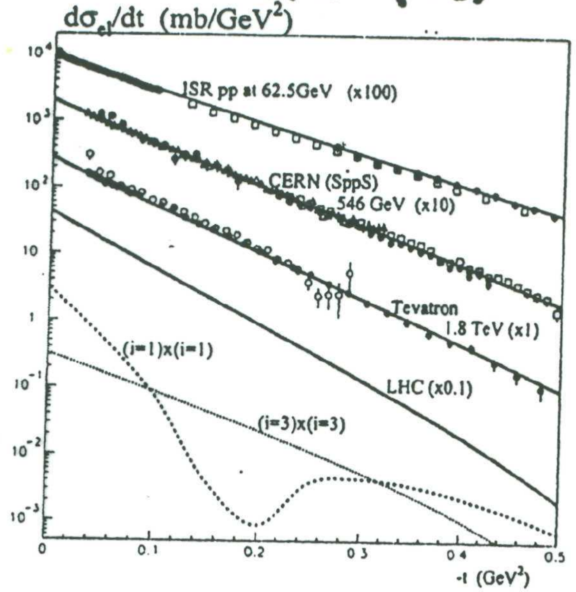

$\Delta_{I\!P} = 0.30 \quad \alpha'_{I\!P} = 0.05$

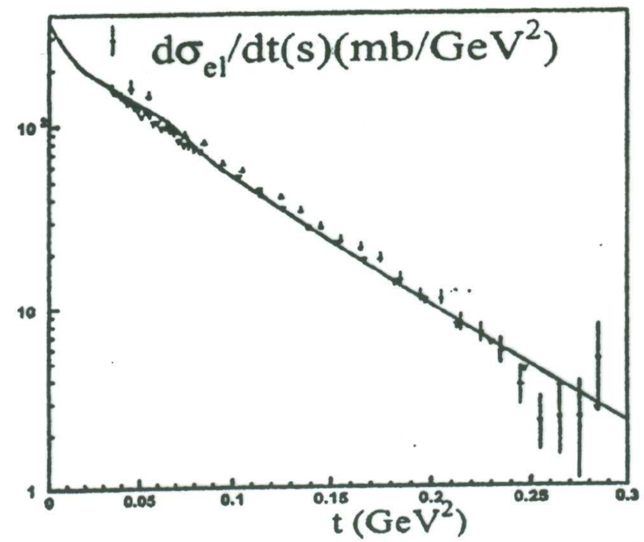

GLMM(08) GW

$\Delta_{I\!P} = 0.12$

$\alpha'_{I\!P} = 0.012$

GLMM(08) GW+$I\!P_{enh}$

$\Delta_{I\!P} = 0.335$

$\alpha'_{I\!P} = 0.010$

LKMR(08)

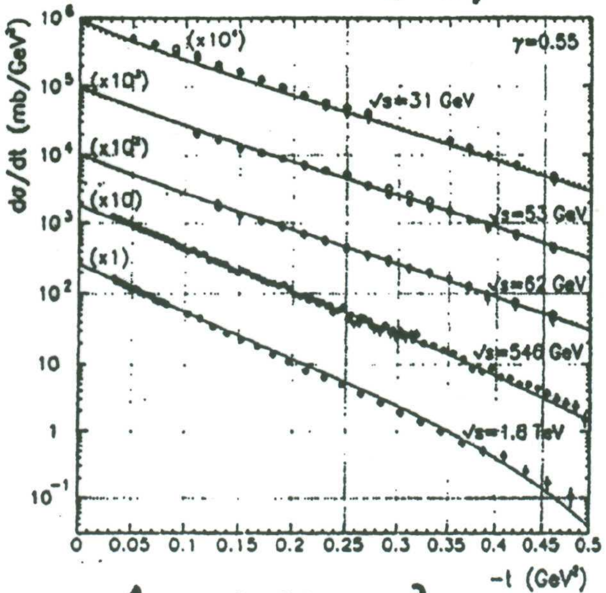

$\Delta_{I\!P} = 0.121 \quad \alpha'_{I\!P} = 0.033$

The extensive LKMR(09) analysis of $\frac{d\sigma_{sd}}{dt\, d\frac{M^2}{s}}$ convincingly demonstrates the need to supplement the $3\mathbb{P}$ vertex with secondary Regge Contributions such as $\mathbb{P}\mathbb{P}\mathbb{R}$ and $\mathbb{R}\mathbb{R}\mathbb{P}$. However, LKMR model does not address the $\mathbb{P}$ enhancement contribution. As such this analysis has very limitted relevance in our context.

Once again, the less extensive analysis of KMR(07) and GLMM(08) is a consistency check as both model need an arbitrary background term to reproduce the CDF data. Note, also, that LKMR were able to fit the CDF $\frac{d\sigma_{sd}}{dt\, d\frac{M^2}{s}}$ at 540 and 1800 GeV only after a relative normalization rescale of 25%.

To conclude: in as much as I admire KMR for their intuition, I do not think that their data analysis provides convincing support to their theoretical assumptions and numerics of their parameter choice.

$$1 - x_L = \frac{M_{sd}^2}{s}$$

GLMM(08) $\mathbb{P}$ enhanced + GW

$\Delta_P = 0.335 \quad \alpha'_{\mathbb{P}} = 0.010$

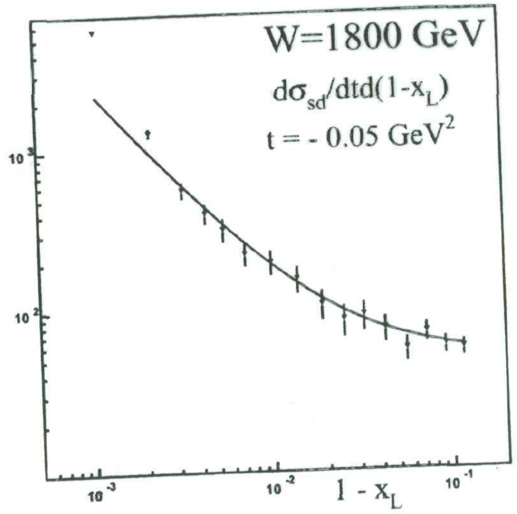

LKMR(08)

GW +

Mueller's $3\mathbb{P}$ SD only

$\Delta_{\mathbb{P}} = 0.121 \quad \alpha'_{\mathbb{P}} = 0.033$

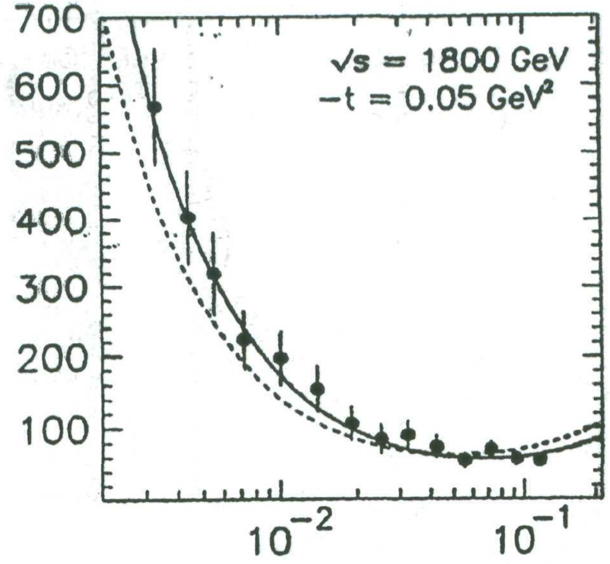

KMR(07)

$\mathbb{P}$ enhanced + GW

$\Delta_{\mathbb{P}} = 0.55 \quad \alpha'_{\mathbb{P}} \equiv 0$

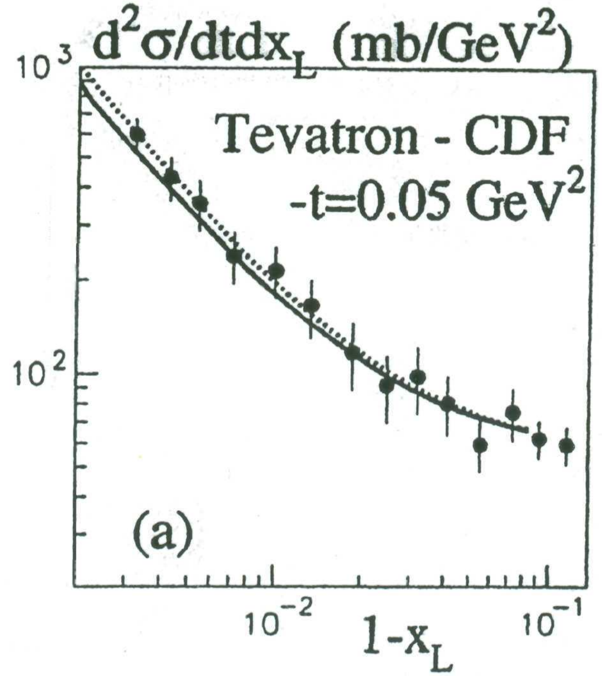

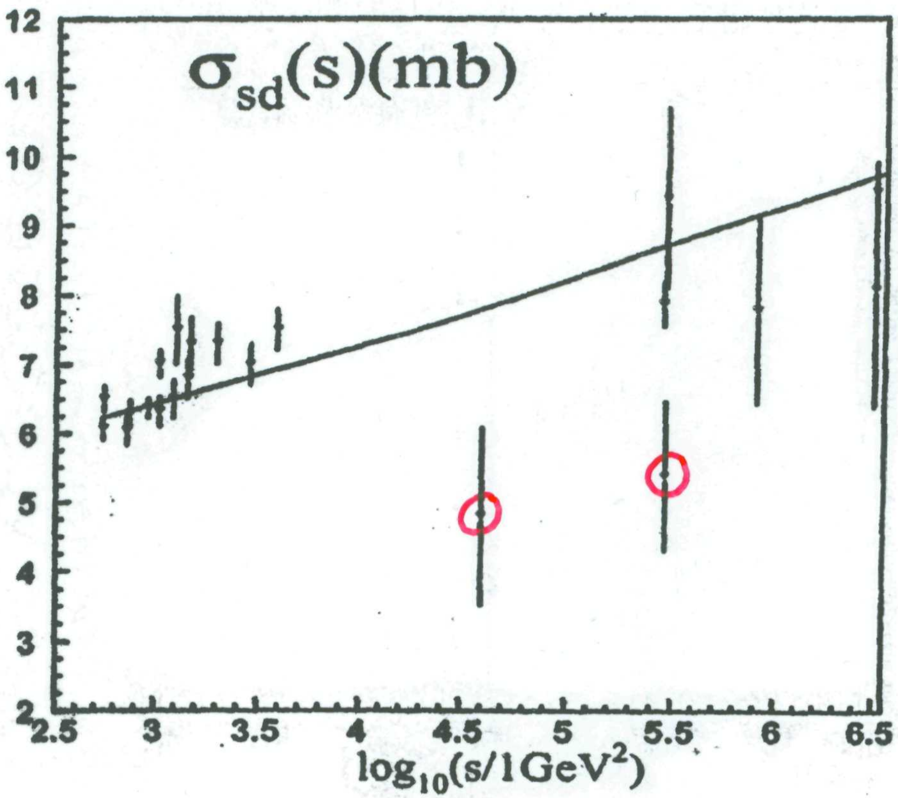

Checking the SD cross section reproduction in GLMM(08) we encounter the old problem that there is no unique algoritm defining diffraction.

Never the less, even with this problematic set of data points we were able to re-fit the IP parameters and GW amplitudes with reasonable margins of errors.

As a test of the stability of our output we have repeated our fitting where the above set of data points was replaced by Goulianos-Montanha corrected set of cross sections and got the same output with smaller errors.

6. Survival Probabilities

My discussion will be confined to a Standard Model Higs (or dijets) with a low mass of 120 – 160 GeV produced in an exclusive central diffraction at the LHC: $p + p \to p + LRG + H(2J) + LRG + p$

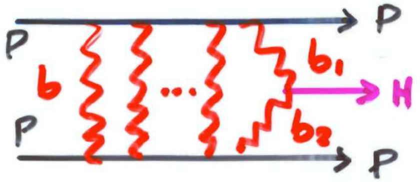

The advantage of this channel is that it has a distinctive signature of 2 LRG and a favorable signal to background ratio, which is improved when the forward protons are tagged.

The hard pQCD calculation of this cross section is reduced by an s-channel unitarity suppression which is manifested by the re scatterings of the incoming colliding projectiles. Given the hard amplitude this suppression (survival probability is naturally calculated in the eikonal model).

$$S^2_{2ch} = \frac{N(s)}{D(s)}$$

$$N(s) = \int d^2b_1\, d^2b_2 \,\{(1 - a_{el}(s,b))\, A_H^{pp}(b_1)\, A_H^{pp}(b_2) - a_{sd}(s,b)\left(A_H^{pd}(b_1)\, A_H^{pp}(b_2) + A_H^{pp}(b_1)\, A_H^{pd}(b_2)\right) - a_{dd}(s,b)\, A_H^{pd}(b_1)\, A_H^{pd}(b_2)\,\}^2$$

$$\underset{\sim}{b} = \underset{\sim}{b_1} + \underset{\sim}{b_2}$$

$$D(s) = \int d^2b_1\, d^2b_2 \,\{A_H^{pp}(b_1)\, A_H^{pp}(b_2)\}^2$$

The calculation of S^2_{2ch} requires a knowledge of the pre screened diffractive (i,k) amplitudes. GLMM did not calculate these amplitudes. Our calculation requires just the non screened diffractive (hard) slopes which we obtain from HERA J/ψ photoproduction and DIS. Even though KMR have calculated the non screened Higgs production diagram, they did not utilized their own resuelts. Their method is very similar to ours, though some what simpler, as they consider just J/ψ photoproduction where as we include also the J/ψ inelastic slope. Note that originally we used an old edition of J/ψ slope data. With the updated HERA data our results are about 30% higher

	W= 1.8 TeV	W=14 TeV
GLMM	3.2 − 5.3 %	2.35 − 4.6 %
KMR	2.7 − 4.8 %	1.2 − 3.2 %

Calculated S^2_{2ch}

GLMM and KMR calculations of S^2_{2ch} are compatible with a small systemic difference traced to $g_1 \simeq g_2$ in KMR while $g_2 \gg g_1$ in GLMM. The overall cross section reduction has two components $S^2_H = S^2_{2ch} \times S^2_{enh}$ where, S^2_{enh} is induced by multi Pomeron interactions. The assumed factorization of S^2_H needs clarification:

As we saw the calculation of S^2_{2ch} maintains a "soft-hard factorization" in as much as there is no contact between the initial soft rescattering and the final non GW diffraction.

The $\mathbb{P}$-enh. sector has 2 different contributions:

1) $\mathbb{P}$ connecting the "hard" two interacting Pomerons which lead to central diffraction. This contribution is contained in GLMM (08). It is not included in any of the KMR versions of S^2_{enh}.

2) $\mathbb{P}$ conecting the incoming projectiles with the "hard" interacting Pomerons. This contribution breaks the factorization of "soft-hard". originally, both GLMM and KMR considered this suppression to be very small, hence its neglect by GLMM. In the recent set of their publications, KMR estimate this contribution to be $S^2_{enh}(KMR) = \frac{1}{3}$. This is an average!

LHC

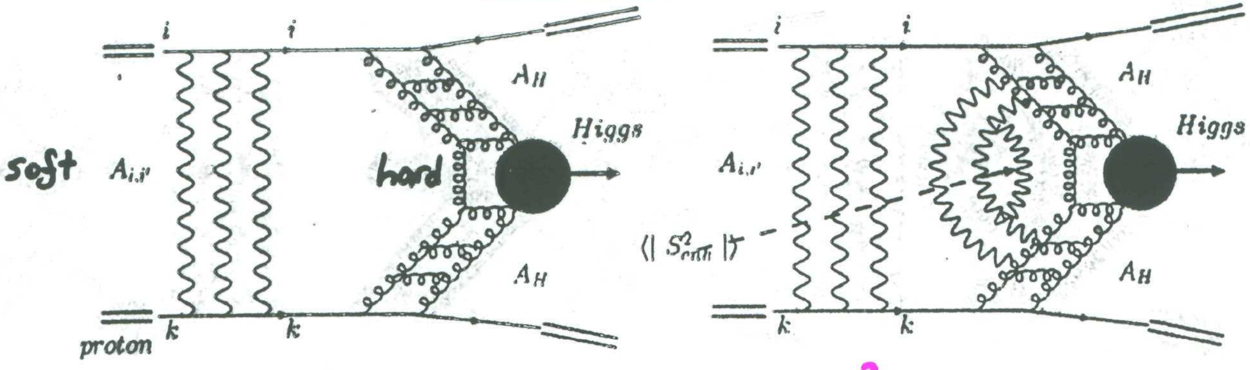

GLMM (08)

factorizable soft-hard

$S^2_H = 0.0025$ $\quad$ $S^2_{\mathbb{P}\,enh} = 0.063$ $\quad$ $S^2_{2ch} = 0.04$

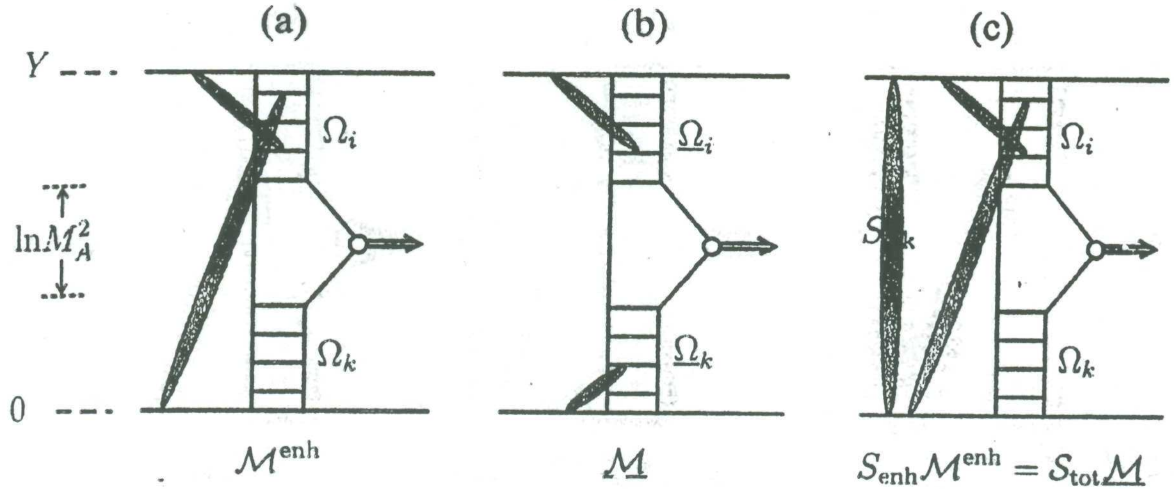

KMR (08)

soft-hard non factorizable

$S^2_H = 0.015$ $\quad$ $S^2_{\mathbb{P}\,enh} = 0.33$ $\quad$ $S^2_{2ch} = 0.045$

As noted, we distinguish in the calculations of multi Pomerons between enhanced and sei-enhanced diagrams. In the enhanced sector we have even number of $3\mathbb{P}$ couplings. In the semi enhanced the numer can be either even or odd. The semi enhanced diagrams are critical in diffractive channels.

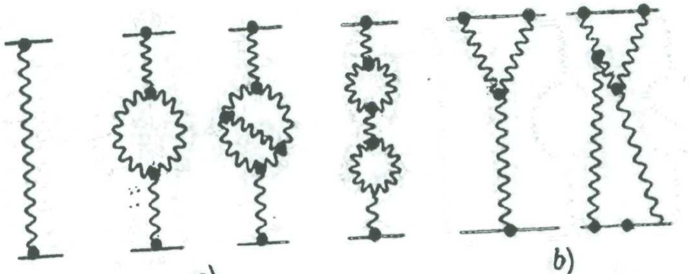

enhanced   semi enh.

GLMM calculation of $S^2_{enh.}$ takes into account only the enhanced diagrams.

Our preliminary suggests that summing also over the semi enhanced diagrams does not change S^2_{enh} significantly.

Recall, that the semi enhanced contribution to SD and DD was added by hand order by order.

KMR summed over the enhanced and semi enhanced diagrams in their soft cross section calculations. I am not clear from their presentations if their S^2_{enh} calculation includes the semi enhanced diagram. None of their published diagrams or text refer to this issue.

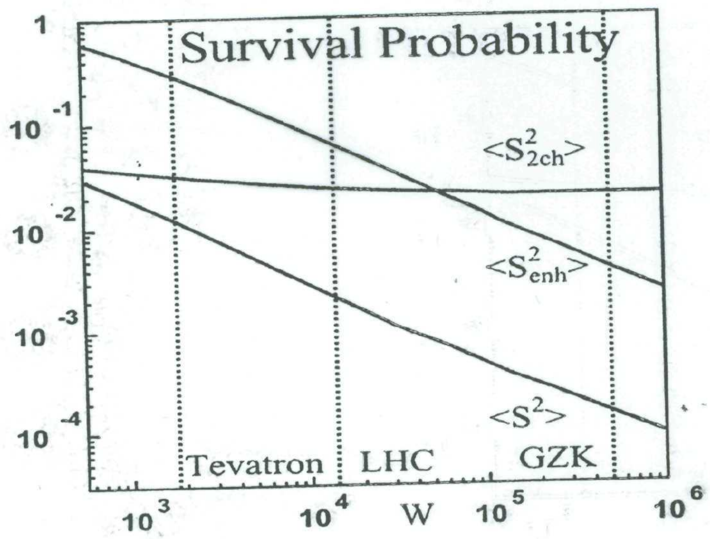

Figure 18: Energy dependence of centrally produced Higgs survival probability.

LRG final state in pp collisons initiated by vector bosons (γ, Z, W) are susceptible to S^2_{2ch} reduction, taking into account their particular b-dependence. S^2_{enh} is not relevant in these reactions.

To summarize:

$$\frac{S^2_H(\text{KMR})}{S^2_H(\text{GLMM})} = \begin{cases} 1.8-3.2 & : \text{Tevatron} \\ 4.8-6.0 & : \text{LHC} \end{cases}$$

The gap between the two sets of S^2_H calculated values originates mostly from the non compatability of the predicted values of S^2_{enh}.

Note the difference between the energy dependence of S^2_{2ch} and S^2_{enh} in GLMM. In KMR both S^2_{2ch} and S^2_{enh} have a very mild energy dependence.

7. The Approach Toward the Black Disc Bound

The unitarity bound $|A_{i,k}(s,b)| \le 2$ holds if $\Omega_{i,k}(s,b)$ is arbitrary. In the eikonal model $\Omega_{i,k}$ is real, i.e. $A_{i,k}(s,b)$ is imaginary. The small real part of $A_{i,k}(s,b)$ can be calculated utilizing dispersion relations (Cauchy theorem). In this case the unitarity bound coincides with the black disc bound $|A_{i,k}(s,b)| \le 1$.

It is easy to see that $A_{i,k}(s,b) = 1$ if and only if

$$A_{1,1}(s,b) = A_{1,2}(s,b) = A_{2,2}(s,b) = 1.$$

This implies that $a_{el}(s,b) = 1$ while $a_{sd}(s,b) = a_{dd}(s,b) = 0$.

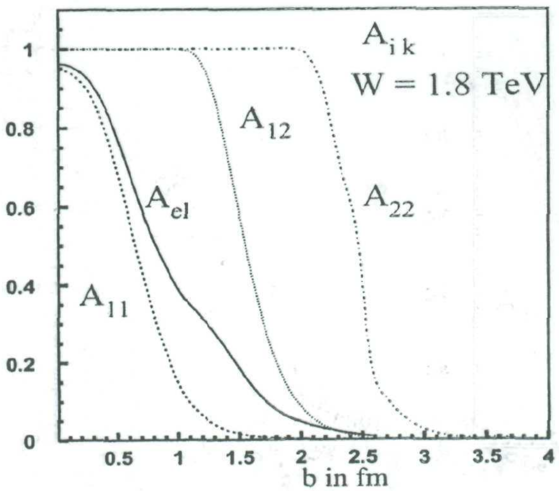

Fig. 14-a

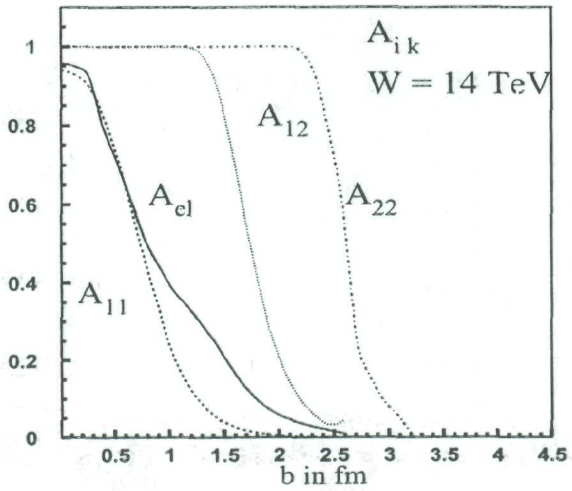

Fig. 14-b

Figure 14: Impact parameter dependence of $A_{i,k}$ and a_{el} at different energies.

As a result the integrand of the convolution defining $S^2_{2ch}(s)$ at this b vanishes

$$S^2_{2ch}(s,b) = 0$$

The interest in the rate at which $a_{el} \to 1$ at small b is obvious as a feature of conceptual interest. Lets discuss its details.

- Recall that if $a_{el}(s,b)=1$ all diffractive channels (soft or hard) vanish at this (s,b) point, be it a consequence of the GW mechanism properties or because $S^2_{2ch}(s,b)=0$.
- Checking the GLMM(08) fitted parameters it is clear that since $g_2 \gg g_1$, $A_{2,2}(s,b=0)$ reaches unity at relatively low energies, $A_{1,2}(s,b=0)$ reaches unity at medium $W \simeq 100$ GeV and $A_{1,1}(s,b=0)$ will reach unity at exceedingly high energies well above LHC. So would $a_{el}(s,b=0)$.
- In KMR(08) $g_1 \simeq g_2$ and consequently in this model $a_{el}(s,b=0)$ will reach unity just above the LHC energy.
- We expect that even though σ_{tot} and σ_{el} as calculated by the two models at LHC and Auger are comparable $S^2_{2ch}(GLMM) > S^2_{2ch}(KMR)$. Recall, that the adjusted values of $A_{i,k}$ are determined in GLMM(08) by a fit to a GW + $\mathbb{P}$-enh. model.

The behaviour of $R_D = \frac{\sigma_{el} + \sigma_{sd} + \sigma_{dd}}{\sigma_{tot}}$ conveys information on the onset of s-unitarity constraints at high energies. Assume that diffraction originated exclusively from the GW mechanism. We obtain then the Pumplin bound: $R_D \le \frac{1}{2}$. The non GW multi Pomeron induced diffractive contributions are not included in the Pumplin bound since they originate from $G^{in}_{i,k}$ rather than from $A_{i,k}$. As such they are reduced from their non screened calculated rates by the corresponding survival probability. The delicate balance between the increase of the non screened cross section and the decrease of S^2 with energy is model dependent. In GLMM(08) $R_D < 0.5$ decreasing slowly with energy. In KMR(07) $R_D > 0.5$ increasing slowly with energy up to $W = 10^5$ GeV which is the high energy limit of validity for both KMR and GLMM. The origin of the KMR prediction is the relatively fast increase of high mass diffraction.

8. Conclusions

	Tevatron			LHC			W=10^5 GeV		
	GLMM	KMR(07)	KMR(08)	GLMM	KMR(07)	KMR(08)	GLMM	KMR(07)	KMR(08)
σ_{tot}(mb)	73.3	74.0	73.7	92.1	88.0	91.7	108.0	98.0	108.0
σ_{el}(mb)	16.3	16.3	16.4	20.9	20.1	21.5	24.0	22.9	26.2
σ_{sd}(mb)	9.8	10.9	13.8	11.8	13.3	19.0	14.4	15.7	24.2
$\sigma_{sd}^{\text{low M}}$	8.6	4.4	4.1	10.5	5.1	4.9	12.2	5.7	5.6
$\sigma_{sd}^{\text{high M}}$	1.2	6.5	9.7	1.3	8.2	14.1	2.2	10.0	18.6
σ_{dd}(mb)	5.4	7.2		6.1	13.4	?	6.3	17.3	
$\frac{\sigma_{el}+\sigma_{diff}}{\sigma_{tot}}$	0.43	0.46		0.42	0.53	?	0.41	0.57	
S^2_{2ch}(%)	5.3	1.8-4.8		4.0	1.2-3.2	4.5	3.45	0.9-2.5	
S^2_{enh}(%)	28.5	100		6.3	100	33.3	3.3	100	
S^2(%)	1.5	2.7-4.8		0.25	1.2-3.2	1.5	1.15	0.9-2.5	

TABLE III: Comparison of GLMM, KMR(07) and KMR(08) outputs.

- GLMM (08) and KMR (07,08) outputs of σ_{tot}, σ_{el}, $\frac{d\sigma_{el}}{dt}$ are compatible. The recent edition of KMR(08) results on the above is very close to ours.
- KMR (07,08) estimates of high mass diffraction are higher than ours. The difference gets larger with increasing energy. σ_{dd}(KMR) at high masses was not published in KMR(08) recent edition.
- S^2_H (KMR(08)) $\simeq 6\, S^2_H$ (GLMM(08)). Most of the incompatability stems from high mass diffraction attributed to multi-Pomeron int.